Carbohydrate Polymers 96 (2013) 31–38

Contents lists available at SciVerse ScienceDirect

Carbohydrate Polymers

journal homepage: www.elsevier.com/locate/carbpol

Hydration and mechanical properties of arabinoxylans and β-D-glucans films

Ruifeng Ying[a], Corinne Rondeau-Mouro[a,1], Cécile Barron[b], Frédéric Mabille[b], Annick Perronnet[c], Luc Saulnier[a,*]

[a] UR1268 Biopolymères, Interactions, Assemblages, INRA, F-44316 Nantes, France
[b] UMR 1208 "Ingénierie des Agropolymères et Technologies Emergentes", INRA – CIRAD – UMII – Supagro, F-34000 Montpellier, France
[c] Université de Nantes, CRTT, UMR GEPEA, CNRS 6144, UNAM, 37 Bd de l'Université, BP 406, 44602 St-Nazaire Cedex, France

ARTICLE INFO

Article history:
Received 4 January 2013
Received in revised form 20 March 2013
Accepted 26 March 2013
Available online 3 April 2013

Keywords:
Wheat
Cereals
Polysaccharide films
Effective moisture diffusivity
Cell walls
TD-NMR
Mechanical properties

ABSTRACT

Arabinoxylans (AX) and (1 → 3)(1 → 4)-β-D-glucans (BG) are the main components of the cell walls in the endosperm of wheat grain. The relative occurrence of these two polysaccharides and the fine structure of the AX are highly variable within the endosperm. Films of AX and BG were used as models of the cell wall to study the impact of polymer structure on the hydration and mechanical properties of the cell walls. Effective moisture diffusivities (D_{eff}) of AX and BG films were determined from 0 to 95% relative humidity (RH) at 20 °C. D_{eff} was influenced by the water content, and the structure of polysaccharides. Higher D_{eff} was obtained for films made with highly substituted AX compared to values obtained for films made with BG or lowly substituted AX. Proton dipolar second moments M_2 and water T_2 relaxation times measured by TD-NMR, indicated that the highly branched AX films exhibited a higher nano-porosity, favoring water motions within films. Results from traction tests showed significant different mechanical properties between the AX and BG films. BG films exhibited much higher extensibility than AX films. Strength and extensibility of AX films decreased with increasing arabinose to xylose ratio. Our results show that the water motions and the mechanical properties of AX and BG films can be linked to the polysaccharide chains interactions that modulate the nanostructure of films.

1. Introduction

The cell walls of cereal endosperm account for 0.02–0.04 g/g dry weight basis (d.b.) of this tissue but have a significant effect on wheat grain uses (milling, bread-making, and brewing), in animal feeding or in human nutrition (Fincher & Stone, 1986). In wheat endosperm, arabinoxylans (AX) and (1,3)(1,4)-β-D-glucans (BG) are the main components of the cell walls (Saulnier, Sado, Branlard, Charmet, & Guillon, 2007).

AX are formed of a linear backbone of (1,4)-linked β-D-xylopyranosyl (Xylp) residues to which single α-L-arabinofuranosyl (Araf) residues are attached on positions O-3 (mono-substitution) and O-3/O-2 (di-substitution). In addition a small proportion of arabinosyl residues are esterified on position O-5 by ferulic acid. Variations in the structure of AX that affects the overall arabinose substitution and the proportion of mono- and di-substitution levels are observed. These structural variations are roughly described by the arabinose to xylose ratio (A/X) that varies from 0.3 up to 1 (Saulnier et al., 2007).

(1,3)(1,4)-β-D-glucans, commonly known as β-D-glucans or β-glucans, are linear homopolymers of D-glucopyranosyl residues linked mostly via two or three consecutive β-(1,4) linkages that are separated by a single β-(1,3) linkage (Cui, Wood, Blackwell, & Nikiforuk, 2000; Dais & Perlin, 1982). Longer segments of consecutively β-(1,4) linked D-Glcp residues represent less than 10% of the molecule and are mainly constituted by oligomers with a degree of polymerization (DP) of 5 and 6. There is no evidence that two or more adjacent β-(1,3) linkages occur in the BG chains (Burton & Fincher, 2009).

Dramatic changes occur in endosperm cell wall composition with respect to both the relative occurrence of individual constituents (AX and BG) and the fine structure of AX according to grain development and localization of cell walls within grain (Jamme et al., 2008; S. Philippe, C. Barron, P. Robert, M. F. Devaux, L. Saulnier, L., & F. Guillon, 2006; S. Philippe, P. Robert, C. Barron, L. Saulnier, & F. Guillon, 2006; S. Philippe, L. Saulnier, & F. Guillon, 2006; Philippe, Tranquet, Utille, Saulnier, & Guillon, 2007; Robert et al., 2011; Saulnier et al., 2009; Toole et al., 2007; Toole et al., 2010). The relationships between structural variation of polymers such as the level of substitution of AX and cell wall properties are not explained and

* Corresponding author. Tel.: +33 2 40 67 50 62; fax: +33 2 40 67 50 66.
E-mail address: luc.saulnier@nantes.inra.fr (L. Saulnier).
[1] Current address: Irstea, UR TERE, 17 avenue de Cucillé, CS 64427, 35044 Rennes, France.

0144-8617/$ – see front matter © 2013 Elsevier Ltd. All rights reserved.
http://dx.doi.org/10.1016/j.carbpol.2013.03.090

the biological significance of this structural diversity is not understood.

During its development up to the final desiccation stage at maturity, the grain water content decreases from 60% down to 12–14%. However, this average value masks water content differences in the various endosperm regions of the mature and developing grain, as already shown by NMR imaging in barley (Glidewell, 2006). In this respect, the changes in cell wall polymer structure observed during the grain development and within the grain tissue could possibly modulate the hydration properties of the cell walls and contribute to regulate the water content of the grain. In this context, we have prepared films of AX or BG and used them as a "model" of the endosperm cell walls in order to study the possible impact of the fine structure of the polymers on the hydration properties of cell walls.

BG and water-extractable AX with high, middle and low A/X ratios were isolated and used to prepare films in controlled conditions. The impact of the polymer structure on water diffusivity and mobility in the films were then studied using dynamic vapor sorption (DVS) and TD-NMR spectroscopy. The mechanical properties of AX and BG films were also determined using traction tests at different relative humidity values corresponding to the water content observed during grain development.

2. Materials and methods

2.1. Materials

Water-extractable AX were prepared by graded ethanol precipitation from wheat flour water extract, as described by (Dervilly, Saulnier, Roger, & Thibault, 2000). Three pure AX fractions exhibiting contrasted arabinose to xylose ratios (A/X: 0.33, 0.53 and 0.73) were isolated and used for further experiments. For clarity, these samples were encoded AX33, AX53 and AX73. Water soluble β-D-glucans from barley (medium viscosity, purity >97%) were purchased from Megazyme and are named BG thereafter.

2.2. Chemical and physicochemical analyses

The method of Englyst and Cummings was used to determine the monosaccharide composition (Englyst & Cummings, 1988; R. Ying, L. Saulnier, & C. Rondeau-Mouro, 2011). Ferulic acid content in AX was determined by UV spectroscopy as described by (Saulnier et al., 1999). Weight average molecular weight (M_w), and intrinsic viscosity ([η]) were determined using high-performance size exclusion chromatography (HPSEC) as previously described (R. Ying, C. Barron, L. Saulnier, & C. Rondeau-Mouro, 2011).

2.3. Film preparation and characterization

AX and BG were dissolved in water (20 mg/mL) and 5 mL of polysaccharide solution was poured into polystyrene Petri dishes (Ø 5 cm). Then, Petri dishes were put in a climate room at 40 °C and 40% relative humidity (RH) for 3 days, as previously described (R. Ying, C. Barron, et al., 2011). Reflectance spectroscopy (SPECORD S600) was used to determine film thickness at 20 °C and 40% RH. (Goodman, 1978)

2.4. Microstructure of films

Films were observed at room temperature (around 20 °C) and around 40% RH using a scanning electron microscope (SEM-Zeiss EVO®MA10) working at 15 kV, 30 Pa for examination of film surface or 5 kV, 4.63 Pa × 10^{-4} Pa for examination of transverse section of film. The film surface was also investigated by atomic force microscopy (AFM) using an Autoprobe CP Park Scientific Instrument (Sunnyvale, CA). AFM images were recorded in the intermittent contact mode using beam-shaped phosphorous-doped silicium cantilevers (Veeco Probes, CA) with a quoted spring less than 50 N/m and that were excited at a frequency proximate to a resonant frequency of around 280 KHz. Sample surfaces were scanned with the probe at a scanning frequency of 1 Hz. Each sample was investigated at least in five different areas with different magnifications. Samples were observed at room temperature (around 20 °C) and around 40% RH. The root mean square (RMS) roughness (R) was defined as follows:

$$R = \sqrt{\frac{\sum_{n=1}^{N}(z_n - \bar{z})^2}{N-1}} \quad (1)$$

where $\bar{z}$ is the average of the z values (height) within the given area, z_n is the current z value, and N is the number of data points within the given area.

2.5. Water sorption isotherms and effective diffusivity using DVS

A controlled atmosphere microbalance DVS apparatus (Surface Measurement System Ltd., London, UK) was used to determine the water sorption kinetic of AX and BG films at 20 °C at relative humidity (RH) ranging from 10 to 95%. Duplicate experiments were carried out for all samples, as previously described (R. Ying, C. Barron, et al., 2011).

Sorption isotherms were fitted by the Brunauer–Emmett–Teller (BET) and the Guggenheim–Anderson-de–Boer (GAB) models. The BET model (Eq. (2)) is commonly used to model sorption isotherms up to 50% RH while GAB (Eq. (3)) has been used for the modeling up to 80% RH. The parameters used in both models, such as m_{0BET}, m_{0GAB}, C_{BET}, C_{GAB} and K_{GAB}, provide information related to the monolayer value and the sorption energies involved during the sorption process (Al-Muhtaseb, McMinn, & Magee, 2002; Brunauer, Emmett, & Teller, 1938; Chirife & Iglesias, 1978; Timmermann, 2003).

$$M = \frac{m_{0BET} C_{BET}(p/p_0)}{(1-p/p_0)(1-p/p_0 + C_{BET}p/p_0)} \quad (2)$$

M in BET model (Eq. (2)) is the moisture content (% dry weight basis, d.b.), m_{0BET} monolayer value (% d.b.), C_{BET}, a temperature dependent constant (related to the net heat of sorption at the monolayer), and p/p_0 the water vapor partial pressure or relative humidity at thermodynamic equilibrium.

$$M = \frac{m_{0GAB} C_{GAB} K_{GAB}(p/p_0)}{(1-p/p_0)(1-K(p/p_0) + C_{GAB}K(p/p_0))} \quad (3)$$

M in GAB model (Eq. (3)) is the moisture content (% d.b.), m_{0GAB} monolayer value (% d.b.), C_{GAB} a constant related to the energy associated to the binding of the sorbant molecules at the monolayer, K_{GAB} related to the heat of sorption at the multilayer, and p/p_0 the water vapor partial pressure or relative humidity at thermodynamic equilibrium.

Models for moisture transport and for sorption isotherms were simulated using MATLAB software (The Mathworks Inc, Natick, Mass., USA.). The GAB and BET equations parameters and the moisture diffusivity values were identified using Levenberg Marquardt method from experimental sorption kinetics by minimizing the root mean square of the deviations between simulated and experimental results as follows (Williams & Mittal, 1999):

$$RMSE = \sqrt{\frac{(\hat{y}-y)^2}{(N-p)}} \quad (4)$$

where $\hat{y}$ is the vector of the predicted values (g/g d.b.), y is the vector of the experimental values (g/g d.b.), N is the number of terms in the

predicted or experimental vector, and p the number of estimated parameters.

Effective water diffusitivity D_{eff} was determined according to the Fick's second law and samples were considered as a plane sheet of homogeneous thickness with a diameter of 10 mm as previously described (R. Ying, C. Barron, et al., 2011). Thus moisture transfer was only considered in the axial direction. The origin of the x-axis is considered at the interface between the air flux and the film surface. The thickness of the film at different RH was corrected according to moisture content of the films using Eq. (5).

$$L = L_d + \frac{MX}{\rho S} \tag{5}$$

where L is the thickness at given RH, L_d the thickness of the film at RH = 0%, X the moisture content (g/g dry basis), M is the mass of the film, ρ the intrinsic water density, S the surface of the film.

The effective moisture diffusivity was determined using Fick's second law:

$$D_{eff}\left(\frac{\partial^2 X(x,t)}{\partial x^2}\right) = \frac{\partial X(x,t)}{\partial t} \tag{6}$$

where X is the moisture content (g/g d.b.), D_{eff} is the effective moisture diffusivity in the film for a given relative humidity. t is time (s), and x is distance from the interface, that corresponds to the vertical direction in our experiments as previously described (R. Ying, C. Barron, et al., 2011).

2.6. NMR spectroscopy

^{1}H NMR measurements were performed using a time-domain spectrometer (Minispec BRUKER, Germany) operating at a resonance frequency of 20 MHz. Two types of pulse sequences were used. Proton free induction decays (FID) and the Carr–Purcell–Meiboom–Gill (CPMG) pulse sequences (Meiboom & Gill, 1958) as previously described (R. Ying, C. Barron, et al., 2011).

The second moment M_2 values were calculated from the broad part of the FID curve that arose from protons of the solid fraction. The NMR spectrum of these protons is well represented by a combination of a cardinal sinus function and a Gaussian broadening following the Eq. (7) (Abragam, 1961):

$$I_{FID}(t) = A\exp\left(-\frac{a^2\cdot t^2}{2}\right)\frac{\sin bt}{bt} + B\exp(-\frac{t}{T_2^*}) \tag{7}$$

In this equation, the parameters A and B represent the contributions of the immobile and mobile protons in the sample, respectively. The NMR spectrum of the immobile proton fraction is assumed to be a rectangular line shape with a total width $2b$, convoluted with a Gaussian line shape with a standard deviation given by parameter a. The second moment, which is a measure of the strength of the hydrogen's dipolar interactions, is calculated from the fit parameters a and b by the following Eq. (8):

$$M_2 = a^2 + \frac{1}{3}b^2 \tag{8}$$

Transverse relaxation time T_2 were determined using the following models (LeBotlan & Ouguerram, 1997) as previously described (R. Ying, C. Barron, et al., 2011):

$$I_{CPMG}(t) = \sum_{i=1}^{n} A_i \times \exp(-\frac{t}{T_{2i}}) \tag{9}$$

where T_{2i} is the relaxation times of the mobile populations and A_i is the intensity of the mobile populations (Meiboom & Gill, 1958).

2.7. Mechanical tests

Mechanical tests were performed on AX and BG films using a Dynamic Mechanical Thermal Analyser DMTA Mk III (Rheometrics Inc., Piscataway, USA). Humidity control was achieved according to the principle of water vapor saturation at different temperatures. The humidity of samples was controlled with air that was bubbled through water at controlled temperature and that was flushed on the furnace. The temperature of the sample chamber was set at 25 ± 1 °C. Pieces of film (L = 20 mm, l = 2.5 mm) were sampled from Petri dish's films in order to avoid any orientation. The samples were then stored for 3 days at 25 °C at constant relative humidity using saturated salt solutions (RH: 59%, NaBr; RH: 75%, NaCl; RH: 91%, $BaCl_2$). Thickness (22 μm) was checked by reflectance spectroscopy and thickness homogeneity within a serie was controlled by sample weight. Samples were fixed in claws with a gap of 10 mm using a torque wrench (10 cNm). Sample equilibration was followed by a time sweep test at imposed strain (0.1%), (frequency = 10 rad s^{-1}). The sample equilibration was assessed by the stability of elastic modulus (E). Uniaxial tensile tests were performed at a strain rate of 0.001 s^{-1} until rupture. Stress-strain curves were calculated from force-displacement measurements and several rheological parameters were determined:

σ_{ela}: maximum value of the stress in the elastic behavior, (N/mm^2);
σ_{max}: the ultimate stress, or stress to fracture (N/mm^2);
ε_{ela}: the elastic strain corresponding to σ_{ela};
ε_{max}: the ultimate strain, or strain to fracture;
E: the Young modulus, i.e. the slope of the elastic part of the curve (N/mm^2);
W: the total mechanical energy needed to break the sample (J/mm^3).

The energy to fracture (W) was determined from the stress–strain curves, and corresponds to the area under the curves.

The tests in which the samples broke close to the clamps were rejected, to exclude data from samples that might have been damaged during clamping. Results were taken as the average of at least 6 tests (Antoine et al., 2003; Hemery, Mabille, Martelli, & Rouau, 2010).

In order to clearly assess the elastic vs plastic behavior, we used also another mechanical test of loading, unloading cycles at constant strain rate (0.001 s^{-1}).

3. Results

3.1. Polymer and film characterization

AX and BG were characterized for their neutral sugar composition, molar mass and intrinsic viscosity (Table 1). Depending on the degree of substitution and monomer composition the molar mass of the polymer varied between 180 and 280 kD but the intrinsic viscosities of the four polymers were in a similar range (260–330 mL g^{-1}). AX and BG films obtained by casting had homogeneous thickness (22 μm) and AFM (Supplementary material 1) observations confirmed a flat and homogeneous surface with very low roughness values (Root mean square <20 nm). Scanning electron microscopy (SEM) (Supplementary material 2) revealed a very compact structure without micropores or phase separation.

Supplementary material related to this article found, in the online version, at http://dx.doi.org/10.1016/j.carbpol.2013.03.090.

Table 1
Molecular characteristics of arabinoxylans (AX) and β-D-glucans (BG).

	AX33	AX53	AX73	BG
A/X[a]	0.33	0.53	0.73	–
Ferulic acid %[b]	0.23	0.07	0.16	–
uXyl/mXyl/dXyl[c]	76/15/9	68/11/21	56/15/29	–
M_w[d] (g/mol) × 10^{-3}	177.0	196.9	233.2	283.5
$[\eta]$[d] (mL g^{-1})	295.6	284.8	259.6	331.2

Results obtained from duplicates: a: coefficient of variation <4%; b: coefficient of variation <2%; c and d: coefficients of variation <5%.
[a] A/X: arabinose to xylose molar ratio.
[b] Content in g/100 g AX.
[c] In percent of total xylose, uXyl: un-substituted xylopyranose residue; mXyl: xylose residue mono-substituted via O-3 with arabinose; dXyl: xylose residue di-substituted via O-3 and O-2 with arabinose residues.
[d] M_w: weight average molar mass, [η]: intrinsic viscosity.

3.2. Moisture sorption isotherms

The moisture sorption isotherms of the films were determined at 20 °C using a DVS apparatus with RH ranging from 0 to 95% (Fig. 1). The water content (based on the percentage of dry mass) measured in AX films according to RH was in agreement with values previously reported in the literature (Dural & Hines, 1993; Roman-Gutierrez, Mabille, Guilbert, & Cuq, 2003; Zhang et al., 2011). Moisture sorption isotherms of AX and BG films have a classical sigmoidal shape (Fig. 1). For an RH ranging from 10 to 80%, BG films adsorbed more water than the AX films. The behavior of the three AX films was very close but the AX33 adsorbed slightly more water than AX53 and AX73. Above an RH of 90%, an exponential increase in water sorption and an inversion of the behavior of the films were observed, AX53 and AX73 exhibiting a higher water uptake than AX33 and BG films. Similar trends were reported for AX isolated from wheat bran, although above an RH of 80% the water content of AX films (around 0.6–0.7 g/g at RH = 90%) was much higher compared to this study (Zhang et al., 2011). Sorption isotherms were fitted with GAB and BET models and in both cases *RMSE* values were <0.003, showing accurate fits. The monolayer values (Table 2) calculated using GAB model (m_{0GAB}) were 0.08–0.10 g/g for the AX and BG films. Similar values were reported in the literature for films made of starch (Zografi & Kontny, 1986). Monolayer (m_{0BET}) values calculated from the BET model were slightly lower (0.065–0.074 g/g; Table 2). Regardless of the model, the samples are classified in the same way with higher monolayer values for BG and AX33 films compared to AX53 and AX73 films. C_{GAB} and C_{BET} values were higher for BG than for AX films (Enrione, Hill, & Mitchell, 2007a).

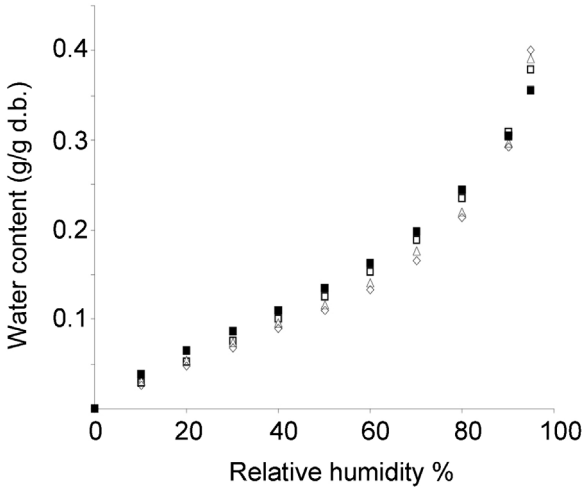

Fig. 1. Moisture sorption isotherm at 20 °C of arabinoxylan and β-D-glucan films (thickness: 22 μm). Filled cubes: β-D-glucan film; open cubes: AX33 film; open diamonds: AX53; open triangles: AX73 film. Vertical bars standing for the experimental error are too weak to be visible on the graph.

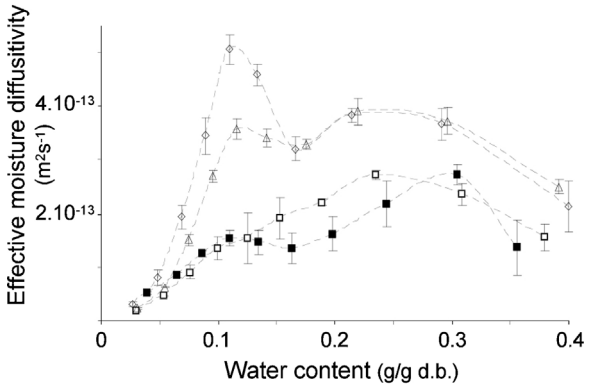

Fig. 2. Effective moisture diffusivity of arabinoxylan and β-D-glucan films as a function of water content at 20 °C. Filled cubes: β-D-glucan film; open cubes: AX33 film; open diamonds: AX53; open triangles: AX73 film.

3.3. Effective moisture diffusivity within films

Effective moisture diffusivity values (D_{eff}) within films were determined at 20 °C using transient-state moisture content of the water sorption kinetics and analytical solution of Eq. (6) for modeling moisture sorption. The diffusivity was assumed to be constant at each RH level (Guillard, Broyart, Bonazzi, Guilbert, & Gontard, 2003). A good fitting of experimental data was observed for each film (Supplementary material 3). The resulting D_{eff} values were plotted in Fig. 2 as a function of moisture content. In general, D_{eff} values were lower at very low and very high water content, and for the intermediate water contents two types of behavior were observed. On one hand, D_{eff} increased sharply as the moisture content increased from 0 g/g to 0.12 g/g for AX53 and AX73 films, and then was nearly constant from 0.12 g/g to around 0.30 g/g. On the other hand, D_{eff} increased slowly from 0 g/g to around 0.30 g/g for AX33 and BG films. In addition, AX53 and AX73 exhibited similar and higher D_{eff} values, than AX33 and BG. The variation of D_{eff} as a function of water content is typical of polysaccharides (Chivrac, Angellier-Coussy, Guillard, Pollet, & Averous, 2010; Enrione, Hill, & Mitchell, 2007b; Yu, Schmidt, Bello-Perez, & Schmidt, 2007) and was also observed for other hydrophilic materials such as cereal-based products (Guillard et al., 2003; Roca, Broyart, Guillard, Guilbert, & Gontard, 2007).

Supplementary material related to this article found, in the online version, at http://dx.doi.org/10.1016/j.carbpol.2013.03.090.

3.4. TD-NMR and mobility of molecules

Fig. 3A shows the effects of the water content on M_2 values measured for AX and BG films. As previously described (R. Ying, L. Saulnier, et al., 2011) M_2 depends on two contributions: first the intramolecular dipolar interactions between protons, modulated by local proton mobility and their inter-distances within molecules (within polysaccharide chains), and second the intermolecular dipolar interactions between protons dependent on chain motions and average distance between the polysaccharide chains. At 20 °C, AX (whatever the substitution ratio) and BG films at water content below 0.05 g/g were characterized by very high and similar M_2 values (>7.10^{+9} rad^2 s^{-2}), then M_2 decreased as water content increased (Fig. 3A). The high and similar values of M_2 for AX and BG films at very low water content (<0.05 g/g) indicated that motions of the polysaccharide chains were very reduced. The decrease of

Table 2
values of GAB and BET models for arabinoxylan (AX) and β-D-glucan (BG) films.

	GAB (modeled up to 80% RH)				BET (modeled up to 50%RH)		
	Monolayer $m_{0\ GAB}$ (% d.b.)	C_{GAB}	K_{GAB}	RMSE	Monolayer $m_{0\ BET}$ (% d.b.)	C_{BET}	RMSE
AX33	10.2 ± 0.8	5.2 ± 1.1	0.76 ± 0.02	0.001	7.2 ± 0.2	6.9 ± 1.4	0.002
AX53	8.1 ± 0.1	5.8 ± 0.2	0.81 ± 0.00	0.002	6.5 ± 0.1	6.6 ± 0.1	0.002
AX73	8.5 ± 0.2	6.9 ± 0.8	0.79 ± 0.00	0.001	6.5 ± 0.1	8.9 ± 1.1	0.002
BG	10.0 ± 0.3	7.6 ± 0.6	0.76 ± 0.01	0.001	7.4 ± 0.1	10.6 ± 0.9	0.002

RMSE: root mean square error; RH: relative humidity.
AX33: AX with arabinose to xylose ratio of 0.33; AX53: AX with arabinose to xylose ratio: of 0.53; AX73: AX with arabinose to xylose ratio of 0.73.

M_2 as a function of the water content, reflects the decreasing of the dipolar interaction strengths. At water content higher than 0.20 g/g the molecular motions of polysaccharide chains become important averaging any intermolecular proton interactions and giving rise to the loss of "non random" structures (Abragam, 1961; Van den Dries, Besseling, van Dusschoten, Hemminga, & van der Linden, 2000). The values of M_2 for AX53 and AX73 films were lower than for AX33 and BG films for the same water content above 0.05 g/g. This result indicates higher proton dipolar interactions within AX33 and BG films in relation with shorter inter-proton distances between polysaccharide chains. Fig. 3B shows the increase of water proton relaxation times T_2 of AX and BG films as a function of the water content at 20 °C. At water content below 0.15 g/g, T_2 values for water in AX and BG films were similar (0.82–0.89 ms) and low, then increased sharply at water content above 0.15 g/g.

As already described(Belton, 2011), the understanding of the behavior of water in low water content biopolymer systems is really challenging. The proton relaxation times measured in such a system have to be analyzed by taking into account the types of protons contributing to the signal and the exchange mechanisms with biopolymers. Previous results (R. Ying, L. Saulnier, et al., 2011) have emphasized that in AX and BG films, the water spin–spin relaxation times T_2 depended on the temperature and the water content of films. Interpretation of the T_2 values and their ratio compared to the total signal (including the solid fraction from polysacharides) has been proposed by considering complementary mechanisms involving the mobility of the polysaccharide chains both below and above the glass transition temperature, and the mobility of water molecules in chemical exchange with the hydroxyl groups of the polysaccharides. In spite of the complexity of these mechanisms, it was found that AX films displayed higher T_2 values than BG films at water content above 0.15 g/g suggesting that the rotational mobility and exchange of water were slower in BG films (R. Ying, L. Saulnier, et al., 2011).

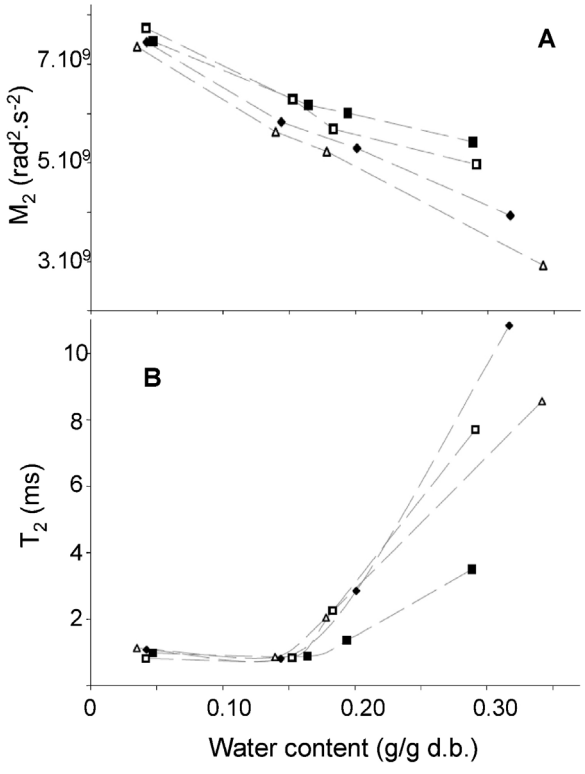

Fig. 3. Effect of the water content at 20 °C on the second moment M_2 (A) and on the water relaxation time T_2 (B) for arabinoxylan (AX) and β-D-glucan (BG) films. Filled cubes: β-D-glucan film; open cubes: AX33 film; open diamonds: AX53; open triangles: AX73 film. Vertical bars standing for the experimental error are too weak to be visible on the graph.

3.5. Mechanical properties of AX and BG films

AX and BG films showed an elastoplastic behavior as commonly observed for plant tissue (Fig. 4) (Köhler, 2000). The main mechanical parameters of the films at different moisture content are shown in Table 3.

Mechanical properties were strongly modified by the water content, as usually observed for hydrophilic polymer (Hemery et al., 2010) where water acts as a plasticizer. Young's modulus decreased significantly as the water content increased from 0.15 to 0.30 g/g, as well as the ultimate stress (10 times lower) and fracture energy (30 times lower). The plastic strain of AX and BG films did not change significantly, from 0.15 to 0.18 g/g, but then decreased sharply at higher water content (0.18–0.30 g/g). The slope of the plastic part of the curve decreased when the water content of the films increased indicating that the break is more due to the stress than the strain effect.

Mechanical properties were also highly modified by the polymer structure as previously observed for AX films (Hoije, Sternemalm,

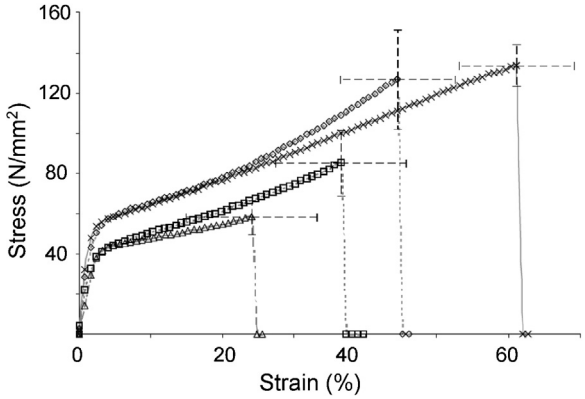

Fig. 4. Typical stress-strain curves obtained during a tensile test with arabinoxylan and β-D-glucan films. Experimental data at relative humidity 59%; cross: β-D-glucan films; diamonds: AX33 films; cubes: AX53 films; triangles: AX73 films (arabinose to xylose ratio: 0.73).

Table 3
Influence of the water content of arabinoxylan (AX) and β-D-glucan (BG) films on their glass transition temperature (T_g) and mechanical properties.

	Water content (d.b.)	T_g (°C)	Elastic strain (%)	Stress at elastic limit (N/mm^2)	Young modulus (N/mm^2)	Ultimate strain (%)	Ultimate stress (N/mm^2)	Rupture energy (J/mm^3)
BG	0.1643	101.6	1.6 ± 0.4	52.7 ± 3.8	3340 ± 363	62.5 ± 8.0	124.5 ± 10.3	54.0 ± 9.8
	0.1940	70.9	2.4 ± 0.6	32.7 ± 2.2	1410 ± 260	65.4 ± 12.0	73.8 ± 9.0	36.4 ± 11.3
	0.2886	29.1	–	–	712 ± 226	15.8 ± 2.8	19.5 ± 2.6	2.9 ± 0.7
AX33	0.1524	82.9	1.8 ± 0.3	54.5 ± 8.5	2926 ± 717	45.6 ± 8.0	131.4 ± 24.7	39.3 ± 9.5
	0.1832	58.7	2.2 ± 0.1	31.8 ± 7.8	1403 ± 355	38.9 ± 10.3	77.7 ± 24.1	20.6 ± 10.5
	0.2911	7.5	–	–	461 ± 136	8.3 ± 2.3	12.6 ± 1.5	1.1 ± 0.4
AX53	0.1439	84.9	1.8 ± 0.2	45 ± 4.0	2475 ± 255	38.6 ± 9.1	97.6 ± 16.2	25.9 ± 8.4
	0.1802	57.9	2.3 ± 0.5	28.1 ± 2.6	1175 ± 323	37.2 ± 7.6	59.2 ± 8.8	15.1 ± 4.4
	0.3169	11.9	–	–	325 ± 133	7.2 ± 3.3	8.1 ± 4.5	0.7 ± 0.4
AX73	0.1396	81.6	2.2 ± 0.2	46.6 ± 8.9	2111 ± 359	21.7 ± 9.2	61.0 ± 8.5	11.1 ± 5.4
	0.1782	56.1	2.3 ± 0.4	26.6 ± 5.4	1155 ± 253	9.5 ± 4.2	26.7 ± 12.1	2.4 ± 1.3
	0.3417	−6.0	–	–	263 ± 119	11.9 ± 5.6	6.5 ± 3.8	0.7 ± 0.6

AX33: AX with arabinose to xylose ratio of 0.33; AX53: AX with arabinose to xylose ratio: of 0.53; AX73: AX with arabinose to xylose ratio of 0.73.

Heikkinen, Tenkanen, & Gatenholm, 2008). Differences were more pronounced at low water content (0.15 g/g – around 0.18 g/g), whereas at water content around 0.30 g/g significant differences remained only between BG and AX. BG films are stiffer (Young modulus) and more extensible than AX films. The ultimate stress of BG and AX33 films were similar (125–130 N/mm^2; water content 0.15 g/g), and significantly higher than highly substituted AX53 and AX73 films (60–98 N/mm^2, water content 0.15 g/g). As previously reported for AX with a slightly different A/X range (0.2–0.5) (Hoije et al., 2008) a higher A/X ratio corresponded to both lower ultimate stress and ultimate strain.

The plastic part of the curves exhibited similar slopes (120–130 N/mm^2, water content 0.15 g/g) until 25% of strain for all polymers. Then, AX33 and AX53 films showed a slight increase of this slope above 20–30% of strain until break (Fig. 4), while no change was observed for BG films.

Fig. 5 shows BG and AX33 film's stress-strain histories generated using unloading and reloading test. The shape of the stress-strain curve of BG film is similar to continuous loading test but the cyclic test gave higher ultimate strain (1.45 ± 0.16 at water content around 0.18 g/g). BG films exhibited similar ultimate stress with the two methods, thus the slope of the non-reversible part of the curve decrease during strain. Between one cycle and the next one, the curve obtained during loading presented three slopes: the first one was the Young modulus, the last one was comparable to plastic phase, and the second one had an intermediate value and reflected a possible polymer rearrangement. Cycle after cycle the first part became smaller, supplanted by the second part. At the opposite, cyclic test on AX33 films exhibited no significant differences in ultimate strain and stress compared to continuous test.

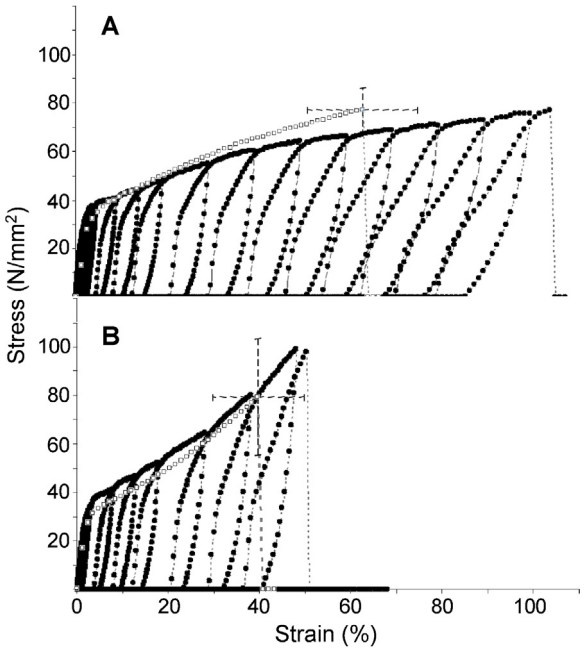

Fig. 5. β-D-glucan (A) and AX33 (B) film stress-strain histories generated using the model of unloading and reloading in tensile at relative humidity 75%. Filled cycles: loading, unloading and reloading cycles in tension of β-D-glucan films, open cubes: continuous loading in tension of β-D-glucan films.

4. Discussion

4.1. Influence of the water content

The increase of the water content highly decreased the strength, stiffness and the glass transition temperatures (Table 3) of the AX and BG films. These observations were correlated with a higher mobility of the polysaccharide chains and an increase of the average distance between polymer chains as determined by NMR. These results confirm that water is a highly efficient plasticizer of amorphous polysaccharides thanks to its ability to interfere with the hydrogen bonding between the carbohydrate chains. Consequently, water can strongly modify the nanostructure of the carbohydrate matrix (Kilburn, Claude, Schweizer, Alam, & Ubbink, 2005). At rubber state (water content around 0.30 g/g at 25 °C), AX and BG films exhibited very low stiffness, strength and extensibility indicating reduced molecular interactions between the polysaccharide chains.

AX and BG films are very dense materials (density = 1500 kg m^{-3}) without macropores (>0.1 μm) that exhibit a very low moisture diffusitivity D_{eff}. However, D_{eff} values increased slightly as a function of the water content. Previous results obtained by TD-NMR and DVS indicated that the variation of D_{eff} could be related to a plasticizing effect of water (R. Ying, C. Barron, et al., 2011). At low water content (below 0.05 g/g) NMR results show a short average distance between the few mobile polysaccharide chains leading to low effective moisture diffusivities. For higher water content, the sorption of water by the carbohydrate matrix improves the mobility of polysaccharide chains and increases the average distances between chains leading to a strong increase of the matrix free volume in both the glassy and rubbery states (Kilburn et al., 2005). This modification of film nanostructure should favor the water diffusion through films.

In addition, the mobility of water molecules measured by NMR can be compared to the D_{eff} values in AX and BG films. In effect, as explained by Belton (2011), the water vapour phase may be a significant mechanism for the transport of polarization and therefore should be considered within the pools of water contributions to the measured T_2 relaxation times.

At water content below 0.15 g/g, T_2 values of water protons in AX and BG films are very low (<1 ms), suggesting that the water is strongly bound to the hydroxyl groups of polysaccharides. At water content above 0.15 g/g, T_2 values increase sharply up to 3.5 ms indicating a higher mobility of water. The increase of mobility (not only rotational mobility but also translational mobility of water)(Van den Dries, Van Dusschoten, & Hemminga, 1998) induced a higher frequency of the water exchanges and an improvement of the desorption of water molecule in the films. Ying et al. (R. Ying, L. Saulnier, et al., 2011) have already proposed that, by increasing the water content within the films, the hydrogen bond stretches and the assembly properties of the polysaccharides weaken while the exchange of water molecules is favored. Therefore, dipolar interactions between water and the hydroxyl groups of the polysaccharides are reduced and the rotational mobility of water is increased. Thus, at high water content, the weak interaction between water and the hydroxyl group of polysaccharides and the high mobility of water also lead to the decrease of D_{eff}.

4.2. Influence of the polysaccharide structures

The structure of the different polymers influences the interaction with water at the molecular level and impacts the diffusion of water and mechanical properties of the films.

The monolayer value (m_0) is of particular interest as it indicates the amount of water strongly adsorbed to specific sites (Karel, 1975). Higher m_0 values were obtained for AX33 and BG films which indicates that these two polymers binds more water than highly branched AX (AX53, AX73). Higher M_2 values were also observed for AX33 and BG films indicating higher proton dipolar interactions and shorter inter-proton distances between polysaccharide chains than for highly branched AX53 and AX73. The higher distance between polysaccharide chains in AX53 and AX73 induces larger free volumes in these films and may explain higher moisture effective diffusivities. Clearly, the interactions between AX chains are decreased by the presence of arabinose side chains leading to higher nano-porosity (Hoije et al., 2008). Compared to AX33, AX53 and AX73 are more highly branched polymers containing 53–73% of arabinose substituents, and a higher proportion of di-substituted residues (21–29% compared to 9% for AX33). The sterical hindrance of disubstituted xylose residues has possibly more impact than mono-substitution on the inter-chain distances.

The results of the tensile tests on films also suggest that mechanical properties of the films could be related to the fine structure of polysaccharides and in particular to the presence of arabinose substituents and especially a high proportion of disubstituted Xyl residues. Lowly substituted AX33 and BG films exhibited similar and higher strength, than highly substituted AX53 and AX73 films. However, while similar M_2 values and film strength were observed for lowly substituted AX33 and BG films, BG films still exhibit a slightly higher extensibility.

The stiffening of AX33 and AX53 films during deformation, suggest that the presence of arabinose residues could stop chains slippage. This side-chain effect gradually leads to an increase in the slope of the plastic part of stress-strain curves for AX33 and AX53 films, and is not observed for smooth BG chains. Cyclic rheological tests also confirmed a different behavior for AX33 and BG films. BG films shows significantly higher extensibility and lower slope of plastic part using classical or cyclic mechanical tests, while AX33 exhibited a similar elastoplastic behavior with a continuous loading of stress under the two conditions. These results are in agreement with the smooth characteristic of BG chains that can easily rearrange during loading while arabinose side-chains distributed along the xylan backbone possibly hamper AX chain rearrangement.

4.3. Impact of the polymer structure on the cell wall properties

Up to now, the relationships between structural variations of polymers such as the level of substitution of AX by arabinose side chains and cell wall properties were not understood. The present work brings new lightning on the possible impact of the polysaccharide structure on the properties of the cell walls in wheat grain endosperm. A higher effective diffusion of water was obtained with highly substituted AX films compared to BG or lowly substituted AX films. In this respect, the different proportions of AX and BG and the variation of the AX structure within the grain endosperm are well correlated with the water properties required for the different cell types in endosperm and their evolution during grain development. AX are more substituted at the beginning of grain filling than at the later stages, suggesting that water diffusion is faster, favoring grain development. Similarly, substitution of AX is higher in the cell walls of the transfer cells that are supposed to play an active role in solute uptake for grain filling. Conversely, moisture diffusivity shall be slower in aleurone cell walls due to its highest thickness, a higher proportion of BG and a lower substitution of AX. During its development wheat grain undergoes dramatic changes in water content and water content decreases from 60% down to 12–14%. Thus, the changes in cell wall polymers structure observed during grain development and within grain tissue could possibly modulate the hydration properties of the cell walls and contribute to regulate the water content of the grain.

In addition mechanical properties of AX and BG films indicated that BG could play an important role on the mechanical and physico-chemical properties of these walls. BG layers are supposed to have a higher extensibility in order to favor the development of cell wall at early stage during the grain development. Compared to the starchy endosperm cell walls at the mature stage of wheat grain development (S. Philippe, C. Barron, et al., 2006; S. Philippe, P. Robert et al., 2006; S. Philippe, L. Saulnier et al., 2006) the high content of BG and lowly substituted AX (around A/X = 0.3) observed in the aleurone cell walls is in line with a higher extensibility and strength of aleurone cell walls.

5. Conclusion

This work confirms that the multi-scale study of polysaccharide films used as models of the polymer lamellar organization in cell walls is an interesting tool to better understand the impact of the polymer structure on cell wall properties in plant tissues. We have demonstrated that the water content and the polymer structure within films can strongly influence interactions between polysaccharides as well as the nanostructure of films. At a higher scale, these changes should significantly impact the moisture diffusion through films as well as their mechanical properties. Our results suggest that the different composition and localization of AX and BG might affect the properties of cell walls in mature grain but also during grain development. Further studies using films made with a mixture of AX and BG (composite films) will improve the model and help to better understand AX-BG interactions in plant cell walls.

Acknowledgments

The authors are indebted to the Regional Council of Pays de la Loire for financial support. V. Guillard and C. Gaillard are greatly acknowledged for helpful discussions. Access to the microscopy

and NMR facilities of the BIBS platform of INRA Angers-Nantes is acknowledged.

References

Abragam, A. (1961). *The principle of nuclear magnetism*. Oxford: Clarendon Press.

Al-Muhtaseb, A. H., McMinn, W. A. M., & Magee, T. R. A. (2002). Moisture sorption isotherm characteristics of food products: A review. *Food and Bioproducts Processing*, *80*(2), 118–128.

Antoine, C., Peyron, S., Mabille, F., Lapierre, C., Bouchet, B., Abecassis, J., et al. (2003). Individual contribution of grain outer layers and their cell wall structure to the mechanical properties of wheat bran. *Journal of Agricultural and Food Chemistry*, *51*(7), 2026–2033.

Belton, P. S. (2011). NMR studies of hydration in low water content biopolymer systems. *Magnetic Resonance in Chemistry*, *49*, S127–S132.

Brunauer, S., Emmett, P. H., & Teller, E. (1938). Adsorption of gases in multimolecular layers. *Journal of the American Chemical Society*, *60*(2), 309–319.

Burton, R. A., & Fincher, G. B. (2009). (1,3;1,4)-D-Glucans in cell walls of the poaceae, lower plants, and fungi: A tale of two linkages. *Molecular Plant*, *2*(5), 873–882.

Chirife, J., & Iglesias, H. A. (1978). Equations for fitting water sorption isotherms of foods: Part 1 – A review. *International Journal of Food Science & Technology*, *13*(3), 159–174.

Chivrac, F., Angellier-Coussy, H., Guillard, V., Pollet, E., & Averous, L. (2010). How does water diffuse in starch/montmorillonite nano-biocomposite materials? *Carbohydrate Polymers*, *82*(1), 128–135.

Cui, W., Wood, P. J., Blackwell, B., & Nikiforuk, J. (2000). Physicochemical properties and structural characterization by two-dimensional NMR spectroscopy of wheat-D-glucan – comparison with other cereal-D-glucans. *Carbohydrate Polymers*, *41*(3), 249–258.

Dais, P., & Perlin, A. S. (1982). High-field, ^{13}C NMR spectroscopy of D-glucans, amylopectin, and glycogen. *Carbohydrate Research*, *100*(1), 103–116.

Dervilly, G., Saulnier, L., Roger, P., & Thibault, J. F. (2000). Isolation of homogeneous fractions from wheat water-soluble arabinoxylans. Influence of the structure on their macromolecular characteristics. *Journal of Agricultural and Food Chemistry*, *48*(2), 270–278.

Dural, N. H., & Hines, A. L. (1993). Adsorption of water on cereal-bread type dietary-fibers. *Journal of Food Engineering*, *20*(1), 17–43.

Englyst, H. N., & Cummings, J. H. (1988). Improved method for measurement of dietary fiber as non-starch polysaccharides in plant foods. *Journal of the Association of Official Analytical Chemists*, *71*(4), 808–814.

Enrione, J. I., Hill, S. E., & Mitchell, J. R. (2007a). Sorption and diffusional studies of extruded waxy maize starch-glycerol systems. *Starch - Stärke*, *59*(1), 1–9.

Enrione, J. I., Hill, S. E., & Mitchell, J. R. (2007b). Sorption behavior of mixtures of glycerol and starch. *Journal of Agricultural and Food Chemistry*, *55*(8), 2956–2963.

Fincher, G. B., & Stone, B. A. (1986). Cell walls and their components in cereal grain technology. *Advances in Cereal Science and Technology*, *8*(8), 207–295.

Glidewell, S. M. (2006). NMR imaging of developing barley grains. *Journal of Cereal Science*, *43*(1), 70–78.

Goodman, A. M. (1978). Optical interference method for approximate determination of refractive-index and thickness of a transparent layer. *Applied Optics*, *17*(17), 2779–2787.

Guillard, V., Broyart, B., Bonazzi, C., Guilbert, S., & Gontard, N. (2003). Moisture diffusivity in sponge cake as related to porous structure evaluation and moisture content. *Journal of Food Science*, *68*(2), 555–562.

Hemery, Y. M., Mabille, F., Martelli, M. R., & Rouau, X. (2010). Influence of water content and negative temperatures on the mechanical properties of wheat bran and its constitutive layers. *Journal of Food Engineering*, *98*(3), 360–369.

Hoije, A., Sternemalm, E., Heikkinen, S., Tenkanen, M., & Gatenholm, P. (2008). Material properties of films from enzymatically tailored arabinoxylans. *Biomacromolecules*, *9*(7), 2042–2047.

Jamme, F., Robert, P., Bouchet, B., Saulnier, L., Dumas, P., & Guillon, F. (2008). Aleurone cell walls of wheat grain: High spatial resolution investigation using synchrotron infrared microspectroscopy. *Applied Spectroscopy*, *62*, 895–900.

Karel, M. (1975). Water activity and food preservation. In M. Karel, O. R. Fennema, & D. B. Lund (Eds.), *Principles of food science. Part II. Physical principles of food preservation* (pp. 237–263). New York; USA: Marcel Dekker, Inc.

Kilburn, D., Claude, J., Schweizer, T., Alam, A., & Ubbink, J. (2005). Carbohydrate polymers in amorphous states: An integrated thermodynamic and nanostructural investigation. *Biomacromolecules*, *6*(2), 864–879.

Köhler, L. (2000). Biphasic mechanical behaviour of plant tissues. *Materials Science and Engineering: C*, *11*(1), 51–56.

LeBotlan, D. J., & Ouguerram, L. (1997). Spin-spin relaxation time determination of intermediate states in heterogeneous products from free induction decay NMR signals. *Analytica Chimica Acta*, *349*(1–3), 339–347.

Meiboom, S., & Gill, D. (1958). Modified spin-echo method for measuring nuclear relaxation times. *Review of Scientific Instruments*, *29*(8), 688–691.

Philippe, S., Barron, C., Robert, P., Devaux, M. F., Saulnier, L., & Guillon, F. (2006). Characterization using Raman microspectroscopy of arabinoxylans in the walls of different cell types during the development of wheat endosperm. *Journal of Agricultural and Food Chemistry*, *54*(14), 5113–5119.

Philippe, S., Robert, P., Barron, C., Saulnier, L., & Guillon, F. (2006). Deposition of cell wall polysaccharides in wheat endosperm during grain development: Fourier Transform-Infrared Microspectroscopy Study. *Journal of Agricultural and Food Chemistry*, *54*(6), 2303–2308.

Philippe, S., Saulnier, L., & Guillon, F. (2006). Arabinoxylan and (1->3), (1 -> 4)-beta-glucan deposition in cell walls during wheat endosperm development. *Planta*, *224*(2), 449–461.

Philippe, S., Tranquet, O., Utille, J. P., Saulnier, L., & Guillon, F. (2007). Investigation of ferulate deposition in endosperm cell walls of mature and developing wheat grains by using a polyclonal antibody. *Planta*, *225*(5), 1287–1299.

Robert, P., Jamme, F., Barron, C., Bouchet, B., Saulnier, L., Dumas, P., et al. (2011). Change in wall composition of transfer and aleurone cells during wheat grain development. *Planta*, *233*(2), 393–406.

Roca, E., Broyart, B., Guillard, V., Guilbert, S., & Gontard, N. (2007). Controlling moisture transport in a cereal porous product by modification of structural or formulation parameters. *Food Research International*, *40*(4), 461–469.

Roman-Gutierrez, A. D., Mabille, F., Guilbert, S., & Cuq, B. (2003). Contribution of specific flour components to water vapor adsorption properties of wheat flours. *Cereal Chemistry*, *80*(5), 558–563.

Saulnier, L., Crépeau, M.-J., Lahaye, M., Thibault, J.-F., Garcia-Conesa, M. T., Kroon, P. A., et al. (1999). Isolation and structural determination of two 5,5'-diferuloyl oligosaccharides indicate that maize heteroxylans are covalently cross-linked by oxidatively coupled ferulates. *Carbohydrate Research*, *320*(1–2), 82–92.

Saulnier, L., Robert, P., Grintchenko, M., Jamme, F., Bouchet, B., & Guillon, F. (2009). Wheat endosperm cell walls: Spatial heterogeneity of polysaccharide structure and composition using micro-scale enzymatic fingerprinting and FT-IR microspectroscopy. *Journal of Cereal Science*, *50*, 312–317.

Saulnier, L., Sado, P. E., Branlard, G., Charmet, G., & Guillon, F. (2007). Wheat arabinoxylans: exploiting variation in amount and composition to develop enhanced varieties. *Journal of Cereal Science*, *46*(3), 261–281.

Timmermann, E. O. (2003). Multilayer sorption parameters: BET or GAB values? *Colloids and Surfaces A: Physicochemical and Engineering Aspects*, *220*(1–3), 235–260.

Toole, G. A., Le Gall, G., Colquhoun, I., Nemeth, C., Saulnier, L., Lovegrove, A., et al. (2010). Temporal and spatial changes in cell wall composition in developing grains of wheat cv. Hereward. *Planta*, *232*(3), 677–689.

Toole, G. A., Wilson, R. H., Parker, M. L., Wellner, N. K., Wheeler, T. R., Shewry, P. R., et al. (2007). The effect of environment on endosperm cell-wall development in Triticum aestivum during grain filling: An infrared spectroscopic imaging study. *Planta*, *225*(6), 1393–1403.

Van den Dries, I. J., Besseling, N. A. M., van Dusschoten, D., Hemminga, M. A., & van der Linden, E. (2000). Relation between a transition in molecular mobility and collapse phenomena in glucose water systems. *The Journal of Physical Chemistry B*, *104*(39), 9260–9266.

Van den Dries, I. J., Van Dusschoten, D., & Hemminga, M. A. (1998). Mobility in maltose – water glasses studied with ^{1}H NMR. *The Journal of Physical Chemistry B*, *102*(51), 10483–10489.

Williams, R., & Mittal, G. S. (1999). Low-fat fried foods with edible coatings: Modeling and simulation. *Journal of Food Science*, *64*(2), 317–322.

Ying, R., Barron, C., Saulnier, L., & Rondeau-Mouro, C. (2011). Water mobility within arabinoxylan and β-glucan films studied by NMR and dynamic vapour sorption. *Journal of the Science of Food and Agriculture*, *91*(14), 2601–2605.

Ying, R., Saulnier, L., & Rondeau-Mouro, C. (2011). Films of arabinoxylans and beta-glucans extracted from cereal grains: Molecular motions by TD-NMR. *Carbohydrate Polymers*, *86*(2), 812–822.

Yu, X., Schmidt, A. R., Bello-Perez, L. A., & Schmidt, S. J. (2007). Determination of the bulk moisture diffusion coefficient for corn starch using an automated water sorption instrument. *Journal of Agricultural and Food Chemistry*, *56*(1), 50–58.

Zhang, Y., Pitkanen, L., Douglade, J., Tenkanen, M., Remond, C., & Joly, C. (2011). Wheat bran arabinoxylans: Chemical structure and film properties of three isolated fractions. *Carbohydrate Polymers*, *86*(2), 852–859.

Zografi, G., & Kontny, M. J. (1986). The interactions of water with cellulose- and starch-derived pharmaceutical excipients. *Pharmaceutical Research*, *3*(4), 187–194.